Edge state, bound state, and anomalous dynamics in the Aubry-André-Harper system coupled to non-Markovian baths

H. T. Cui (崔海涛),[1,2,*] H. Z. Shen (沈宏志),[2,†] M. Qin (秦明),[1] and X. X. Yi (衣学喜)[2,‡]

[1]*School of Physics and Optoelectronic Engineering, Ludong University, Yantai 264025, China*
[2]*Center for Quantum Sciences, Northeast Normal University, Changchun 130024, China*

In this paper, we study bound states and their influence upon the dynamics of a one-dimensional tight-binding system coupled to an environment. We identify three specific kinds of bound states; the first is a discrete bound state (DBS), for which the energy level exhibits a gap from the continuum. The DBS exhibits similar localization features to the edge states of the system and can therefore suppress its decay. The second is a bound state in the continuum (BIC), which can also suppress system decay. The BIC states are found to be strongly connected to the edge mode of the system, since they both show almost the same localization and energy features. The third bound state displays a large gap from the continuum and exhibits extendible (i.e., not localized) behavior. The population of the system in this state decays partially but not entirely, unlike the other bound states. The time evolution of a single excitation in the system is studied to illustrate the influence of the bound states. We find that both the DBS and the BIC play important roles in time evolution; for example, the excitation becomes localized and does not decay depending on the overlap between the initial state and the DBS or the BIC. Furthermore, we observe that the single excitation can show a long-range hopping in a system when the system falls into the strong localizations regime. This feature can be understood by the interplay of system localizations and the bath-induced long-range correlation.

I. INTRODUCTION

In experiments, a quantum system will inevitably interact with its surrounding environment. One typical example is that of solid-state quantum devices, which are frequently disturbed by thermal as well as nonthermal environmental effects. Thus open quantum systems are an important field of study. In addition to exploring environmental effects in quantum devices and shedding light on the boundary between the quantum and classical worlds, the study of open quantum systems may provide a paradigm to interpret how an open system equilibrates with its surroundings. In particular, the localization-delocalization phase transition has been studied intensively in many-body systems with disorder [1,2], and the quantum many-body scarred state has been found to be responsible for the breakdown of thermalization [3,4] when there is no disorder in systems.

Recently bound states with small rates of exponential decay have been reported in open systems [5–7]. These bound states stem from the shift of system-energy levels induced by an emitted photon that pushes the level beyond the cutoff frequency of the environment [6]. As a result of the appearance of an energy gap, the bound states become robust against environmentally induced decays, and prevent quantum systems from thermalizing since the excitations in these states do not equilibrate. The appearance of bound states is a general feature of open quantum systems, independent of their detailed structure. Thus, this provides a general way for systems to prevent decoherence.

Recent experimental explorations of the localization-delocalization transition in cold atomic gases suffer from atom-atom collisions and imperfect trapping [8,9]. The collisions and imperfections can be modeled as environmental factors and the localized phase becomes unstable [9] due to their influence. On the theoretical side, it was shown that the system exhibits a stretched exponential decay when coupled to a Markovian bath [10]; then, the localization is destroyed, and the system is equilibrated. However, the effect of bound states upon the dynamics of open systems as well as on the localization remains unexplored.

In this paper, we will examine the bound states and dynamics of an open system. For concreteness, let us consider a one-dimensional tight-binding atomic chain with onsite modulation, coupled to a bosonic bath. The Hamiltonian of such a chain is

$$H_S = \sum_{n=1}^{N} \lambda(c_n^\dagger c_{n+1} + c_{n+1}^\dagger c_n) + \Delta \cos(2\pi\beta n + \phi)c_n^\dagger c_n,$$

$$(1)$$

where N is the length of the atomic chain, $c_n(c_n^\dagger)$ is the annihilation (creation) operator of excitation at the nth atomic site, and β can be either rational or irrational, characterizing two distinct cases. For brevity, the hopping strength λ is set to be a unit in the following discussion. Thus the physical

---

quantities are automatically scaled in units of λ. For $\beta = p/q$ with p and q being coprime (commensurate case), the edge mode can occur because of the nontrivial topological phase in H_S [11], which leads to the localization of the excitation at the boundary. When β is a Diophantine number [12] (the incommensurate case), H_S corresponds to the Aubry-André-Harper (AAH) model [13], in which a delocalization-localization phase transition occurs when $\Delta = 2$. It has recently been demonstrated that the AAH model is equivalent to a two-dimensional quantum Hall system [14]. Thus a topological edge mode, in which the excitation becomes localized at the boundary, can also be found [14]. Moreover, the AAH model can be realized in cold atomic gases, and experimental exploration of the delocalization-localization phase transition in the AAH model has been intensively pursued [8].

The bath and its coupling to the atomic chain are, respectively, depicted by the following Hamiltonians:

$$H_B = \sum_k \omega_k b_k^\dagger b_k, \quad H_{\text{int}} = \sum_{k,n} (g_k b_k c_n^+ + g_k^* b_k^\dagger c_n),$$

where $b_k(b_k^\dagger)$ is the bosonic annihilation (creation) operator of the kth bath mode, and the frequency $\omega_k \geqslant 0 (\forall k)$. g_k characterizes the coupling strength between the lattice site and the kth bath mode; we assume that the coupling is so weak that the rotating-wave approximation can be applied to H_{int}. Then, the total Hamiltonian is

$$H = H_S + H_B + H_{\text{int}}. \tag{2}$$

Since there is no particle interaction in H_S, the following discussion is restricted to the case of a single excitation, i.e., $\sum_n c_n^\dagger c_n + \sum_k b_k^\dagger b_k = 1$. In this case, the bound state can be determined exactly, and the population dynamics can also be precisely evaluated. Although the particle interaction is important, we do not touch upon it in the current paper, since doing so would make the discussion complicated.

The remainder of this paper is organized as follows. In Sec. II, the definition of a bound state is presented; interestingly a special discrete bound state (DBS) can be found outside of the continuum ω_k, which does not decay and displays similar localization to the edge mode in H_S. However, there also exists a single bound state with very small energy, which is extended and has a certain probability of spontaneous emission. In Sec. III, the population-evolution dynamics are calculated, focusing especially on the interplay between the bound state and localization in the system. It is found that the DBS is dominant in the population-evolution dynamics. Depending on the overlap of the initial state and the DBS, the excitation may become localized against spontaneous emission. Moreover, the bound state in the continuum (BIC) can also be shown to have the same influence on the population-evolution dynamics as did the DBS. The occurrence of a BIC can be attributed to the nontrivial topology of H_S [15,16]. In Sec. IV, the interplay between disorder-induced localization and bath-induced long-range hopping is studied. We note that excitation hopping can occur between distant atomic sites, even if the system is localized strongly; however, such hopping is greatly suppressed when the DBS or the BIC appears. In Sec. V, the long-term behavior of evolution is studied. We observe a very slow decay of excitation in the incommensurate case, even if

the initial state overlaps with the DBS or the BIC. However, this feature is not found in the commensurate case. Finally, the conclusion is presented in Sec. VI.

II. BOUND STATE IN OPEN SYSTEMS

A bound state in open systems is defined as the discrete energy level of the total Hamiltonian [17]. As for $\omega_k > 0$, it corresponds to the negative-energy solutions to the Schrödinger equation:

$$H|\psi_E\rangle = E|\psi_E\rangle. \tag{3}$$

When $E > 0$ the energy solutions can be obtained only for specific ω_k, which therefore constitute a continuum. It is the conventional wisdom that the excitation in the system with eigenvalues that fall within the continuum of the bath would leak and radiate out to infinity. However, a BIC can be found inside the continuum that coexists with extended states, but remains perfectly confined without any radiation [7]. Physically, the occurrence of a BIC can be attributed to level resonance [7]; however, it has recently been shown that the BIC can also be related to the nontrivial topology of the system [15]. To avoid confusion, we refer to the DBS as a discrete energy solution to Eq. (3). With respect to the fact that the BIC can be identified only by the population-evolution dynamics, as shown in Appendix C, the following discussion in this section is only suitable for the DBS.

For a single excitation, $|\psi_E\rangle$ can be expressed generally as

$$|\psi_E\rangle = \left(\sum_{n=1}^N \alpha_n |1\rangle_n |0\rangle^{\otimes(N-1)} \right) \otimes |0\rangle^{\otimes M}$$

$$+ |0\rangle^{\otimes N} \otimes \left(\sum_{k=1}^M \beta_k |1\rangle_k |0\rangle^{\otimes(M-1)} \right), \tag{4}$$

where $|1\rangle_n = c_n^\dagger |0\rangle_n$ denotes the occupation of the nth lattice site, $|0\rangle_k$ is the vacuum state of b_k and $|1\rangle_k = b_k^\dagger |0\rangle_k$, and M denotes the number of the bath mode. Substituting Eq. (4) into Eq. (3), one obtains

$$(\alpha_{n+1} + \alpha_{n-1}) + \Delta \cos(2\pi\beta n + \phi)\alpha_n + \sum_{k=1}^M g_k \beta_k = E\alpha_n, \tag{5a}$$

$$\omega_k \beta_k + g_k^* \sum_{n=1}^N \alpha_n = E\beta_k. \tag{5b}$$

According to Eq. (5b),

$$\beta_k = \frac{g_k^*}{E - \omega_k} \sum_{n=1}^N \alpha_n. \tag{6}$$

Substituting the expression for β_k into Eq. (5a), we obtain

$$(\alpha_{n+1} + \alpha_{n-1}) + \Delta \cos(2\pi\beta n + \phi)\alpha_n$$

$$+ \left(\sum_{k=1}^M \frac{|g_k|^2}{E - \omega_k} \right) \sum_{n=1}^N \alpha_n = E\alpha_n.$$

As for the continuous spectrum ω_k,

$$\sum_{k=1}^{M} \frac{|g_k|^2}{E - \omega_k} \to \int_0^\infty \frac{J(\omega)}{E - \omega} d\omega, \tag{7}$$

where the spectral density is $J(\omega) = \sum_{k=1}^{M} |g_k|^2 \delta(\omega - \omega_k)$. Then one has

$$(\alpha_{n+1} + \alpha_{n-1}) + \Delta \cos(2\pi \beta n + \phi)\alpha_n$$

$$+ \int_0^\infty d\omega \frac{J(\omega)}{E - \omega} \sum_{n=1}^{N} \alpha_n = E\alpha_n. \tag{8}$$

The integral Eq. (7) is divergent for $E > 0$; thus the energy solutions to Eq. (8) can be acquired only for $E < 0$. Physically, the last term on the left-hand side of Eq. (8) characterizes a homogenous hopping of excitation in atomic sites. As will be displayed in Sec. IV, the interplay of this effective long-range correlation and the localization in the system will have a significant effect upon the population-evolution dynamics.

For concreteness, the spectral function is chosen as

$$J(\omega) = \eta \omega \left(\frac{\omega}{\omega_c}\right)^{s-1} e^{-\omega/\omega_c}, \tag{9}$$

where η characterizes the coupling strength between the system and the bath. The bath can be classified as sub-Ohmic ($s < 1$), Ohmic ($s = 1$) or super-Ohmic ($s > 1$) [18]. Equation (9) characterizes the damping movement of electrons in a potential, thus providing a general picture of the dissipation of excitation in the system. When disorder exists, competition between localization and bath-induced dissipation is expected to exert a major influence upon the excitation dynamics. Thus, the choice for $J(\omega)$ is suitable in the current case. As for s, it is shown in Appendix A that the discrete solutions to Eq. (8) negligibly depend on the value of s, except in the ground state. Thus, the following discussion is restricted to the case of $s = 1$. ω_c is the cutoff frequency of the bath spectrum, beyond which the spectral density starts to fall off; hence, it determines the regime of bath frequency, which is dominant for dissipation. In general, the value of ω_c depends on the specific environment. However, as shown in Appendix A, ω_c shows a negligible effect upon the energy solutions to Eq. (8), except in the ground state. Hence $\omega_c = 10$ is chosen to ensure $\Delta/\omega_c < 1$ [18]. In addition, an exceptional case can be found for the minimal solution E_0, which exhibits heavy dependence upon the size of the system and the properties of the bath.

Equation (8) constitutes a linear system of equations for variable α_n. The values of E can be determined by identifying the zero points of the determinant of the coefficient matrix. However, noting that E is also involved in the integrals, one must therefore appeal to numerical considerations. Our evaluation shows that there are at most N negative solutions to E. Consequently, for large N, these solutions constitute a band. In fact we find that the band overlaps significantly with that in H_S for $E \leqslant 0$. This feature can be attributed to weak system-bath couplings: The bath cannot provide sufficient energy for the transition of excitations between different bands. It is difficult to determine the continuous spectrum E numerically. Instead, we try to find a discrete E in the band gap, that is more tractable numerically and interesting in terms
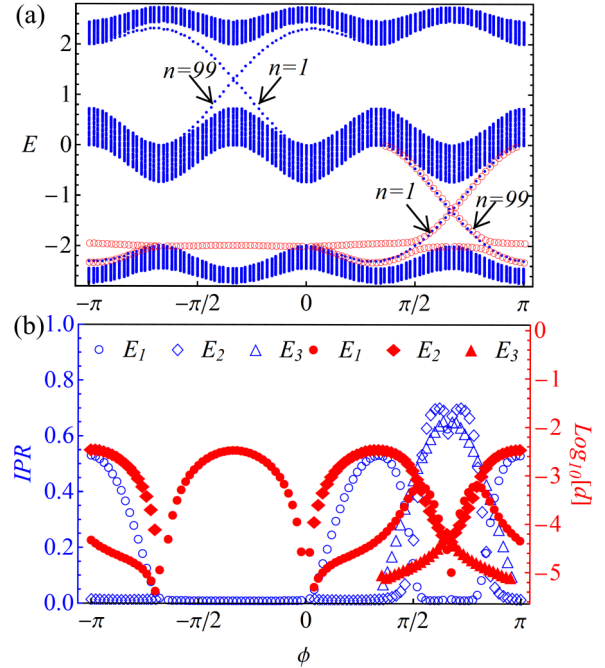

FIG. 1. (a) The plots for the eigenenergy E (in units of λ) of H_S with $\beta = 1/3$ and $\Delta = 2$ (blue point) and the discrete bound states (red empty circle) when $E < 0$. The labels $n = 1(99)$ denote the site at which excitation is localized. (b) Plots of the inverse-participation ratio (empty blue markers) and d (solid red markers) for the DBS in panel (a). The labels E_1, E_2, and E_3 denote the levels of the DBS in increasing order. $N = 99$, $s = 1$, $\eta = 0.1$, and $\omega_c = 10$ are chosen for all plots.

of physics. Moreover the discrete solution is expected to be related strongly to the edge model in H_S, and may be stable against decoherence. Thus, the remaining discussion in this section will focus upon discrete solutions occurring in the gap. The DBS terminology is designated as a special solution here. Two situations are considered separately, namely, the commensurate ($\beta = 1/3$) and incommensurate ($\beta = (1 + \sqrt{5})/2$) cases. As shown in the following discussion, the DBS can behave very differently for these two cases.

A. Commensurate case: $\beta = 1/3$

When $\beta = p/q$ (with p and q being coprime), the spectrum of H_S consists of q bands. As an example, the spectrum of H_S is presented for $\beta = 1/3$ $\Delta = 2$ under the open boundary in Fig. 1(a) (solid points). The edge mode, plotted by discrete solid points in the gap, depicts the localization of the excitation at the ends. By contrast, the state in the band is extended. By solving Eq. (8), three discrete energy solutions at most can be found in the gap for $E < 0$, which are highlighted by red empty circles in Fig. 1(a). It is evident that two different features can be observed for these solutions. One is the DBS that has nearly the same energy as the edge mode in H_S. We find that it exhibits similar localization to the edge state, and can thus be considered to be the renormalization of the edge state. The other is the DBS that has a distinct energy from the edge mode. We find that it is extended instead, as shown by the
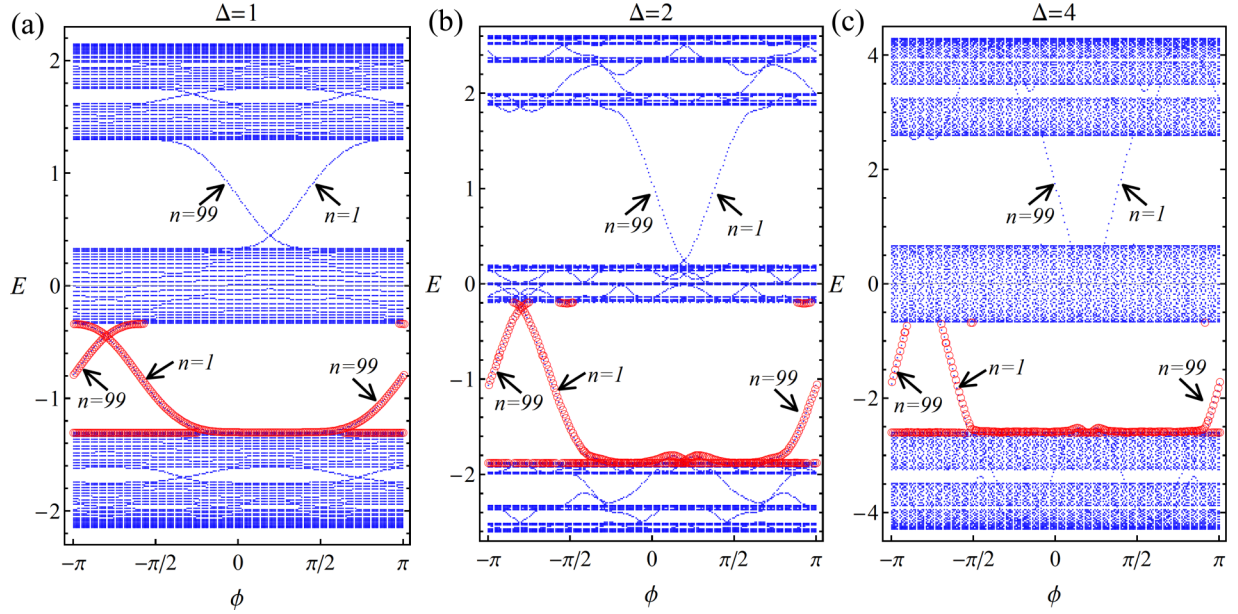
FIG. 2. Plots of the eigenenergy E (solid blue points and in units of λ) of H_S with $\beta = (1 + \sqrt{5})/2$ for (a) $\Delta = 1$, (b) $\Delta = 2$, and (c) $\Delta = 4$, and the DBS for $E < 0$ (empty red circles). The other parameters are the same as those in Fig. 1. The label $n = 1(99)$ denotes the site occupied by the excitation in the edge mode and in the DBS.

inverse-participation ratio (IPR) $\text{IPR} = \sum_n |\alpha_n|^4$ in Fig. 1(b), and thus comes from the transition of the state in the band.

The un-normalized probability of spontaneous emission is defined as

$$d = \sum_k |\beta_k|^2 = \left| \sum_{n=1}^{N} \alpha_n \right|^2 \int_0^\infty \frac{J(\omega)}{(E - \omega)^2} d\omega \qquad (10)$$

and calculated for all the DBSs, as shown in Fig. 1(b), as $\log_{10} d$. Clearly the d has an amplitude not larger than $\approx 10^{-2}$. This picture means that the DBS is robust against spontaneous emission.

However, a single special solution $E_0 \sim 23.13$ can be found for which the corresponding IPR is $\approx 1/99 \approx 0.01$ and the probability of spontaneous emission is ≈ 0.405. Furthermore we also find that E_0 is independent of ϕ and Δ. For example, $E_0 \sim -23.13$ for $\Delta = 1$ and $-23.356 < E_0 < -23.31$ for $\Delta = 4$. Moreover the level E_0 shows significant dependence on the system size N and the bath properties, as shown in Appendix A. Thus this special bound state is extended, and characterizes strong entanglement between the system and the bath.

B. Incommensurate case: $\beta = (1 + \sqrt{5})/2$

The localization-delocalization phase transition can occur when β is a Diophantine number [12]. Given that the Diophantine numbers can be approximated to infinitesimal precision by rational numbers, the system is actually quasiperiodic, which induces a fractal structure in the spectrum of H_S as shown in Fig. 2. Furthermore, there is a critical point $\Delta = 2$ in H_S that separates the delocalized phase ($\Delta < 2$) from the localized phase ($\Delta > 2$). In the delocalized phase all eigenstates tend to be extended, whereas they show

strong localization in the localized phase. The in-gap edge state can also be found under the open boundary condition, since H_S is equivalent to a two-dimensional Hofstadter model [14].

As for concreteness, $\beta = (1 + \sqrt{5})/2$ is chosen. By solving Eq. (8), the DBS can be determined exactly, and is highlighted by red empty circles in Fig. 2 for $\Delta = 1, 2$, and 4, respectively. The spectrum of H_S shows two main gaps as well as several miniature gaps. These fractal gaps stem from the quasiperiodicity in the system, and thus their appearances are sensitive to the size of the system. In this point, the energy solutions in these regions are less meaningful in physics. Consequently the following discussion will focus only upon the solutions in the two main ones. It should be pointed out that we do not try to discuss the variance of critical points because of the coupling to the bath. Thus, the following discussion for $\Delta = 2$ is only to show the influence of the different quasidisorder strengths.

An interesting feature in this case is that the discrete solution in the main gap shows an apparent correspondence to the edge mode. This phenomenon can be attributed to the robustness of quasidisorder against dissipation. Thus no transition occurs for the state in the band, and the edge mode is renormalized as the DBS. Moreover, the localization in the DBS is enhanced with the increment of Δ, as shown by the IPR in Fig. 11 in Appendix B. Furthermore, the corresponding d also tends to disappear, implying that the spontaneous emission of excitation is greatly suppressed.

As in the commensurate case, a single special energy solution E_0 can also be found. For instance, we find that $E_0 \sim -23.13, -23.17$ for $\Delta = 1, 2$ and $\sim -23.351 < E_0 < \sim -25.32$ for $\Delta = 4$. The corresponding $\text{IPR} \approx 0.01$ and $d \approx 0.4$, independent of Δ and ϕ.

C. Further discussion

In a word, the DBS can be found because of the existence of the energy gap and the edge mode in the system. With respect to the strong connection between the DBS and the edge mode, we believe that the occurrence of DBS is a general feature in the AAH model coupled to an environment. A common property for the DBS is the disappearance of spontaneous emission, allowing the excitation to be preserved against decoherence. While the DBS shows one-to-one correspondence to the edge mode in the incommensurate case, an additional DBS can be found in the commensurate one, having distinct energy from the edge mode and behaving in an extended manner, as shown in Fig. 1(a). This phenomenon can be attributed to the quasidisorder in H_S, which makes the system stable against the transition induced by the coupling to a bath. In addition, we also find that the corresponding IPR is smaller than 1, owing to the competition between the disorder-induced localization and the coupling-induced long-range correlation that makes the excitation hop between different sites. A detailed discussion of the IPR can be found in Appendix B.

Another interesting feature is the existence of a special bound state E_0, which is extended and shows a probability of spontaneous emission ≈ 0.4. Moreover this special state exhibits strong dependence on the bath properties and system size N. Consequently E_0 characterizes the equilibrium between localization and dissipation, and is therefore useless for the storage of quantum information.

III. TIME EVOLUTION

The population evolution under a single excitation in the system is discussed in this section to demonstrate the strong influence of the bound state. The evolution equation is written as

$$i\frac{\partial}{\partial t}\alpha_n(t) = [\alpha_{n+1}(t) + \alpha_{n-1}(t)] + \Delta\cos(2\pi\beta n + \phi)\alpha_n(t)$$
$$- i\sum_{n=1}^{N}\int_0^t d\tau\,\alpha_n(\tau)f(t-\tau), \quad (11)$$

where i is the square root of -1, and the memory kernel $f(t - \tau) = \frac{\eta}{\omega_c^{s-1}}\frac{\Gamma(s+1)}{[i(t-\tau)+1/\omega_c]^{s+1}}$ characterizes the relevant correlation function of the bath. Because of the integral, numerical evaluation must be implemented to determine $\alpha_n(t)$. We approach this by rewriting the integrals as a summation with suitable step length. Then, by solving Eq. (11) iteratively, $\alpha_n(t)$ can be determined.

When the bound state occurs, $|\psi(t)\rangle$ can be decomposed into two parts, i.e.,

$$|\psi(t)\rangle = \sum_b \alpha_b|\psi_b\rangle e^{-iE_b t} + \int dE_c\,\alpha(E_c)e^{-iE_c t}|\psi_c\rangle. \quad (12)$$

The summation runs over all bound states $|\psi_b\rangle$ with energy E_b, indicating unitary evolution. The integral over the continuum E_c is responsible for the excitation decay, which tends to vanish after a long time. Hence the bound states will completely determine the final state of the system at long times. To highlight the effect of the DBS or the BIC, we choose the initial state $|\psi(t = 0)\rangle = \sum_n \alpha_n(0)|n\rangle$ with
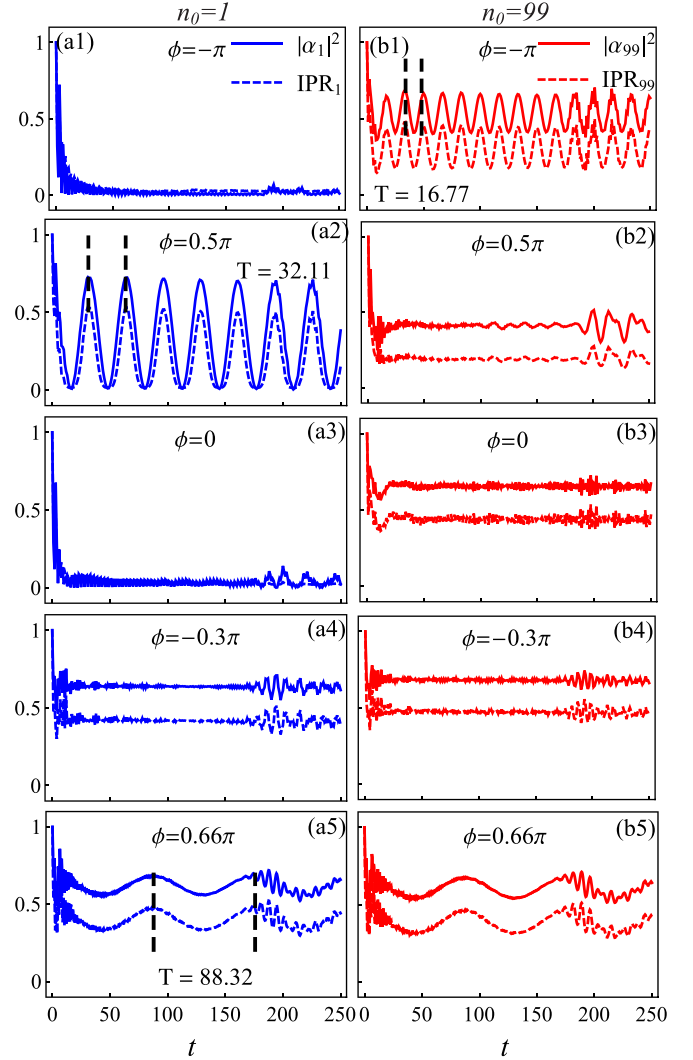

FIG. 3. The evolution of survival probability $|\alpha_n|^2\,(n = 1, 99)$ (solid line) and the corresponding IPR$_n$ (dashed line) for a single excitation initially at $n_0 = 1$ (left column) or $n_0 = 99$ (right column). $\beta = 1/3$ and $\Delta = 2$ are chosen, and the other parameters are the same as those in Fig. 1. The evolution time t is scaled in units of the hopping strength λ.

a single excitation located at atomic sites $n_0 = 1$ and 99, respectively. The corresponding survival probabilities of excitation $|\alpha_1(t)|^2$ and $|\alpha_{99}(t)|^2$ are calculated, together with the corresponding IPR$_{1(99)}$. Three distinct behaviors can be found for the population evolution under a single excitation. First, the excitation becomes localized at its initial site. Then, the excitation can hop to a different site from the initial one. Finally the evolution is dissipative and the excitation can be absorbed by the bath.

A. Commensurate case: $\beta = 1/3$

Five different cases are plotted in Fig. 3. For $\phi = -\pi$, two DBSs can be found when $E < 0$, as shown in Fig. 1(a); one overlaps with the edge state and shows the localization of the excitation at site $n = 99$, whereas the other is extended. It is clear that the survival probability $|\alpha_{99}|^2$ of an excitation

located initially at site $n_0 = 99$ shows a stable oscillation around 0.5, as shown in Fig. 3(b1). This oscillation stems from the interference of two DBSs, and the frequency of oscillation is decided by their energy difference. As shown in Fig. 3(b1), the period of oscillation is $T = 16.77$. Then, $\omega = 2\pi/T = 0.3747$, which is close to the energy difference $\delta E = 0.3768$ of the two DBSs. The slight difference comes from computational error. However, $|\alpha_1|^2$ for $n_0 = 1$ exhibits a rapid decay, as shown in Fig. 3(a1). The same features can also be found for the IPR (dashed line in Fig. 3). This observation implies that the DBS would completely determine the population evolution: When the initial state overlaps with the DBS, the excitation can be preserved with a high probability. If not, the information about the initial state would be erased completely. It should be noted that the weak fluctuation of survival probability for $t > \sim 180$ comes from the accumulation of computational error in solving Eq. (11) iteratively.

Similar phenomena can also be observed for $\phi = 0.5\pi$, in which there are three DBSs, as shown in Fig. 1(a). Two of them show similar localization to the edge states; the third instead exhibits extended behavior. Notably $|\alpha_1|^2$ shows a stable oscillation with period $T = 32.11$ because of the interference of the two lowest DBSs, for which the energy difference is 0.1953. At the same time, $|\alpha_{99}|^2$ also becomes stable because of the DBS with localization at $n = 99$. Another interesting situation is $\phi = 0.66\pi$. There are two DBSs with localizations at sites $n = 1$ and 99, respectively. These are close to each other in energy, as shown in Fig. 1(a). Consequently, a stable oscillation can be found for both $|\alpha_1|^2$ and $|\alpha_{99}|^2$ because of the interference, as shown in Figs. 3(a5) and 3(b5). As will be discussed in next section, this interference induces an end-to-end hopping of excitation.

A special case occurs for $\phi = 0$, in which there is no DBS when $E < 0$. In contrast to the rapid decay of $|\alpha_1|^2$, stable evolution can be observed for the excitation initially located at $n_0 = 99$, as shown in Figs. 3(a3) and 3(b3). This phenomenon can be attributed to the occurrence of the BIC [7], as shown in Appendix C. Generally, the BIC is induced by the level resonance [7]. However, in the present discussion, the BIC can be attributed to the nontrivial topology in H_S [15,16]. Clearly, both the DBS and the BIC influence the population-evolution dynamics in similar ways. Another example of the BIC can be found when $\phi = -0.3\pi$. Under this circumstance, there are two edge states in H_S when $E > 0$, with localization occurring at atomic sites $n = 1$ and 99, respectively. Consequently, both $|\alpha_1|^2$ and $|\alpha_{99}|^2$ show stable evolution, as shown in Figs. 3(a4) and 3(b4).

The localization is enhanced with the increment of Δ, as shown by $|\alpha_{99}|^2$ in Fig. 4 for $\phi = -\pi$. At the same time the evolution of $|\alpha_1|^2$ also becomes stretched slightly. This feature can be attributed to the trapping effect of the onsite potential.

B. Incommensurate case: $\beta = (1 + \sqrt{5})/2$

Two distinct phases can be identified in this case: the delocalized phase ($\Delta < 2$), in which the system is extendible, and the localized phase ($\Delta > 2$), in which the system displays strong localization. As examples, the cases of $\phi = -\pi$ and 0.4π are studied in detail, for which there is a DBS and a BIC with localization at sites $n = 99$ and 1, respectively, as shown
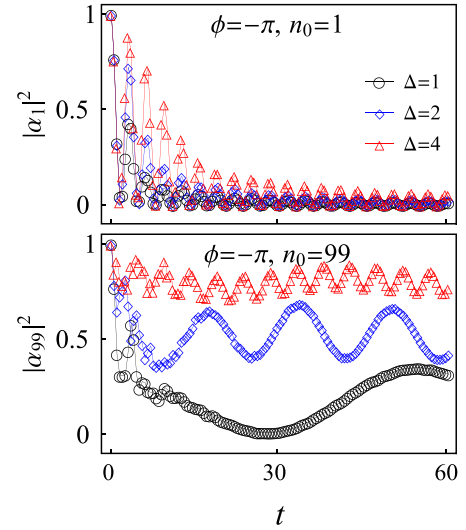

FIG. 4. The plots for the evolution of the survival probability $|\alpha_{1(99)}|^2$ when $\Delta = 1, 2, 4$. $\beta = 1/3$ and $\phi = -\pi$ are chosen. The other parameters are the same as those in Fig. 3.

in Fig. 2. It is expected that a stable evolution can be observed for excitations located initially at $n_0 = 99$ or 1, as shown in Figs. 5(a2) and 5(b1). Furthermore we also note that although the survival probability is enhanced with an increment of Δ a strange feature can be found in Fig. 5(b1), by which $|\alpha_1|^2$ declines smoothly when $\Delta = 4$. This abnormal feature is left for study in Sec. V.

However, the situation becomes different when the initial state does not overlap with any DBS or BIC. For example, the survival probability $|\alpha_1|^2$ for $\phi = -\pi$ exhibits a rapid decay when $\Delta = 1$. However, when $\Delta = 2, 4$, a significant recurrence can be found for $|\alpha_1|^2$, as shown in Fig. 5(a1). This feature can be attributed to the influence of bound states other than the DBS and the BIC. As stated in Sec. II, the solutions to Eq. (8) (other than the discrete ones in the gap) constitute the band, which becomes more localized with increase of
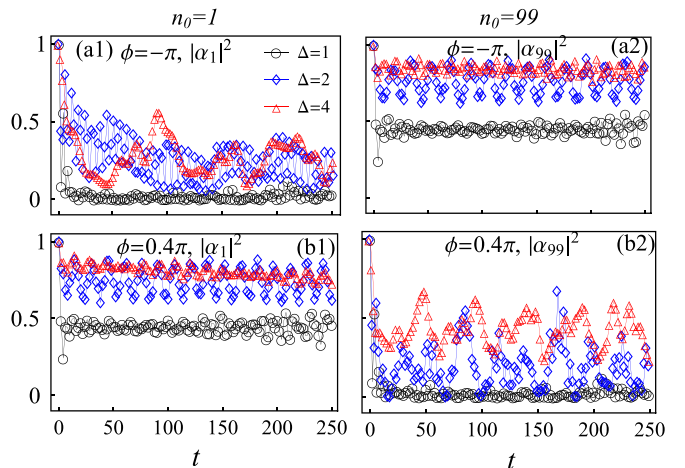

FIG. 5. The plots for the evolution of the survival probability $|\alpha_{1(99)}|^2$ when $\beta = (1 + \sqrt{5})/2$, as well as when $\Delta = 1, 2, 4$. The evolution time t is scaled in units of λ. The other parameters are the same as those in Fig. 3.

Δ. Consequently, when the initial state overlaps substantially with the states in the band, the interference of states would thus induce a temporal revival of $|\alpha_1|^2$. This explanation can be further verified by noting that the recurrence is absent in the commensurate case and when $\Delta = 1$ in the incommensurate case, in which the states in the band are extended or delocalized. A similar picture can also be found for $|\alpha_{99}|^2$ when $\phi = 0.4\pi$, as shown in Fig. 5(b2).

C. Further discussion

It is evident that the occurrence of the DBS or the BIC has a crucial influence on the population evolution of single excitation in systems: Depending on the overlap of the initial state and the DBS or the BIC, the survival probability of the excitation can become stable against dissipation. For both commensurate and incommensurate cases, the excitation can be preserved in the system with a high probability if the initial state overlaps with the DBS or the BIC. If it does not, two different features can be obtained in our discussion. When H_S is commensurate or in the delocalized phase ($\Delta < 2$), the population evolution is dissipative. However, in the localized phase of H_S ($\Delta > 2$), it can show a recurrence due to the strong localization in H_S.

An interesting question is the excitation dynamics when there is no DBS or BIC. As shown by the integral in Eq. (8), an effective long-range correlation in atomic sites is induced by the coupling to the bath, which is responsible for the dissipation of excitation. However, the quasidisorder in H_S tends to localize the excitation within the system. Hence, the interplay of the long-range correlation and the localization by quasidisorder is expected to lead to the exotic excitation dynamics. In the next section, we shed light on the influence of this interplay.

IV. LONG-RANGE HOPPING OF THE EXCITATION

To demonstrate the effects of effective long-range correlation and quasidisorder, the cases $\phi = -0.3\pi$ and 0.7π are considered for $\Delta = 4$. There is no DBS or BIC under these circumstances, as shown in Fig. 2. The survival probability and corresponding distribution of excitation in the system are plotted in Fig. 6. The excitation-occupation probabilities at some sites other than the initial one become pronounced. Meanwhile the evolution of the IPR also becomes complex. This phenomenon results from the interplay of the quasidisorder and the effective long-range correlation: This correlation is responsible for the hopping and dissipation of excitation. On the other hand, the quasidisorder tends to trap and preserve the excitation against dissipation. Consequently, at some moment, the excitation can be maintained with a significant probability at some site, at which the onsite potential is stronger.

However, we find that the hopping can be reduced greatly when a DBS or a BIC appears. For example, we examine the case of $\phi = 0$ when $\beta = (1 + \sqrt{5})/2$, in which there is a BIC with localization at site $n = 99$: For $n_0 = 1$, it is found that the distribution $|\alpha_n|^2 (n \neq 1)$ becomes pronounced at some sites with the increment of Δ, as shown in Fig. 7(b). However, for $n_0 = 99$, it is clear from Fig. 7(b) that $|\alpha_n|^2 (n \neq 99)$ tends
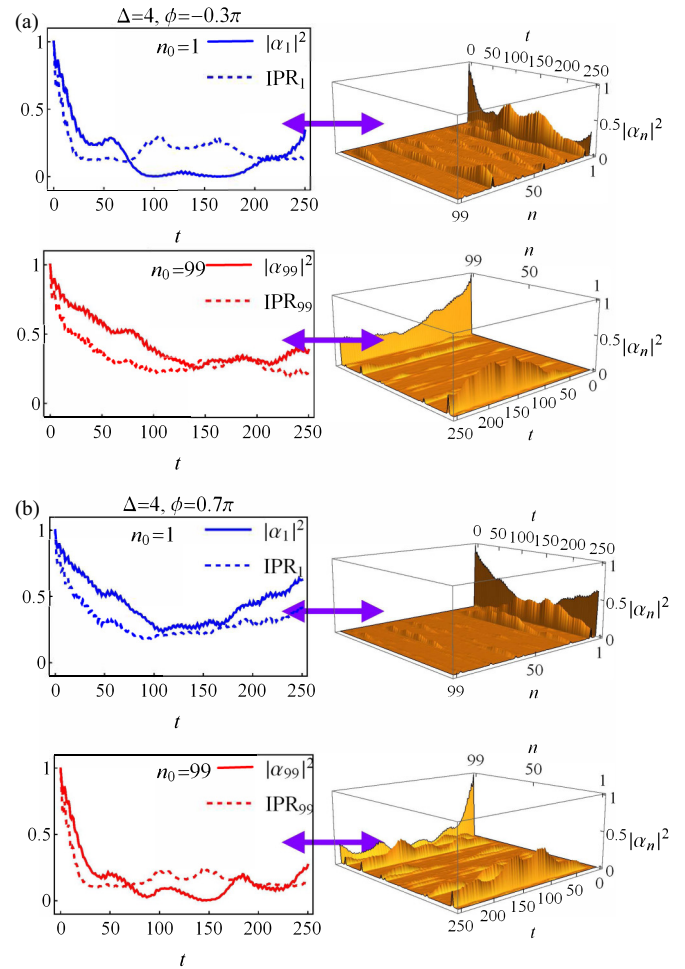

FIG. 6. The plots for the time evolution of survival probability $|\alpha_{1(99)}|^2$, as well as the corresponding IPR$_{1(99)}$, when (a) $\phi = -0.3\pi$ and (b) $\phi = 0.7\pi$. $\Delta = 4$ is chosen, and the other settings are the same as those in Fig. 5.

to disappear even for $\Delta = 4$. This phenomenon originates from the strong localization of the DBS or the BIC, which is protected by the nontrivial topology in H_S.

A similar picture can also be noted in the commensurate case. As shown in Fig. 7(a) for $\phi = 0.66\pi$ when $\beta = 1/3$, excitation hopping can be found *only* between sites $n = 1$ and 99. By contrast, it is absent when there is only one DBS, as shown for $\phi = 0$ in Fig. 7(a).

V. LONG-TERM BEHAVIOR

Although we claim that the DBS or the BIC may determine the steady behavior of the system, it is possible to identify an exception. For $\phi = 0.4\pi$ and $-\pi$ with $\beta = (1 + \sqrt{5})/2$, the survival probability of the excitation declines very slowly when $\Delta = 4$, even if the initial state overlaps with a DBS or a BIC, as shown in Figs. 8(b) and 8(c). We find that this declination cannot be attributed to computational error. By contrast, it does not occur for $\beta = 1/3$, as shown in Fig. 8(a), or for $\Delta = 1$ when $\beta = (1 + \sqrt{5})/2$ shown in Figs. 8(b) and 8(c). For these two cases, the system is extendible or in a delocalized phase. For longer time evolutions, the numerical
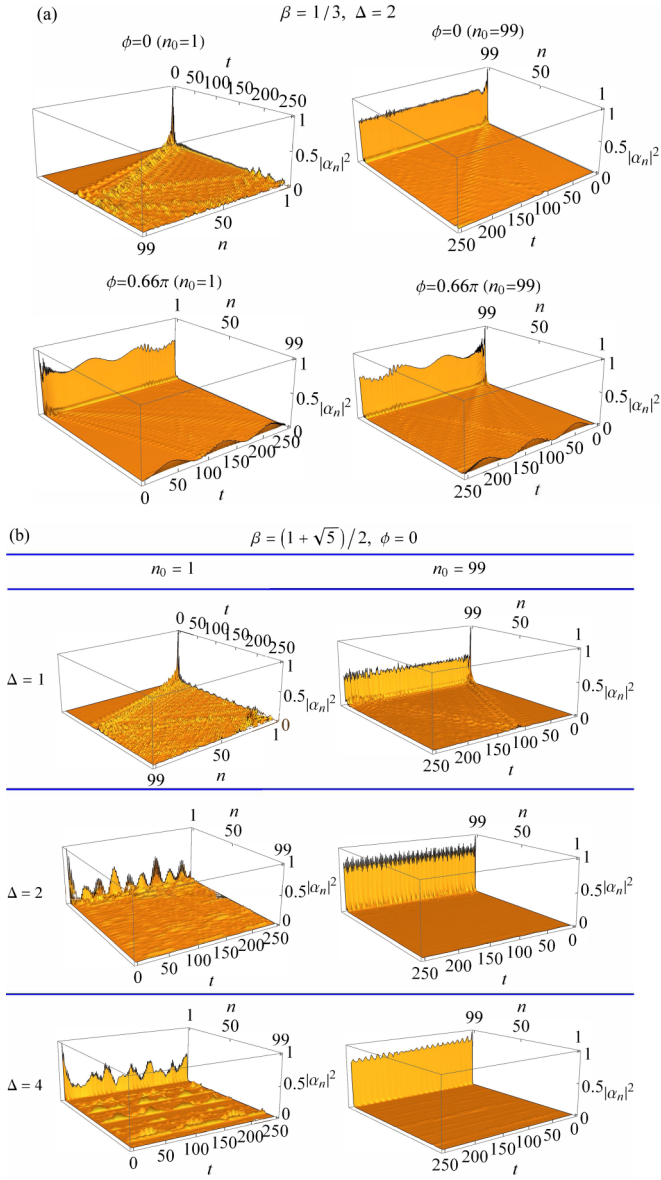
FIG. 7. The plots for the time evolution of $|\alpha_n|^2$ when (a) $\beta = 1/3$ and (b) $\beta = (1 + \sqrt{5})/2$. The chosen values of ϕ and Δ are presented in the plot labels. The other settings are the same as those in Fig. 3 for all plots.
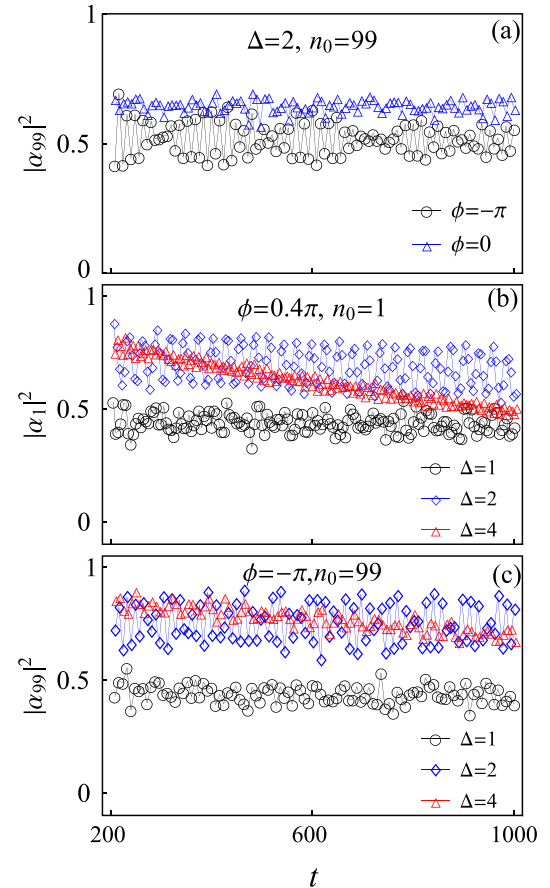

FIG. 8. The plots for the long-term behavior of the survival probability $|\alpha_{1(99)}|^2$ with (a) $\beta = 1/3$ and (b, c) $\beta = (1 + \sqrt{5})/2$. The chosen initial states, as well as ϕ and Δ, are presented by the plot labels. The other parameters are the same as those in Fig. 3.

evaluation becomes exhaustive and thus unreliable, owing to the accumulation of computational error.

Unfortunately, we cannot determine the exact reason for this declination. Given that this phenomenon is absent when the system is extendible or delocalized, one possible explanation may be the influence of the bound states in the band. These states also become much more localized with increasing disorder in H_S. Consequently, they would show a non-negligible contribution to the evolution after a long time.

VI. CONCLUSION

In conclusion, the bound states and their influence upon the population evolution are investigated in a one-dimensional tight-binding atomic chain. Each site of the chain is coupled to the same environment. By solving the Schrödinger equation in the limit of a single excitation, three special kinds of bound states are identified. The first is the DBS, which corresponds to a single negative eigenenergy with a finite gap from the continuum. From the calculations, we conclude that the system with the DBS does not decay, but has similar localization features to the edge mode of the system. An additional DBS is found in the gap when the system is commensurate, which is extendible and can be understood as the bath-induced transition of the state in the band. The situation changes when the system is incommensurate due to the intrinsic localization in the system, preventing it from being excited due to its coupling to the environment.

The second is a bound state in the continuum, which is connected strongly to the edge mode with positive energy and also exhibits a decay rate of zero. The robustness of the BIC could be attributed to the nontrivial topology of the system. The third is a single special bound state of lowest energy. Unlike the first two bound states, it is extendible and displays a certain probability to decay. Moreover it depends sharply upon the size of the system and the properties of the bath.

The time evolution of a single excitation is simulated to explore the influence of the bound states. We conclude that the bound states are dominant for the population evolution.

When the system is extendible or delocalized, the excitation becomes stable against dissipation provided that the initial state overlaps with the DBS or the BIC. However, if the overlapping is zero, the evolution is dissipative, and the information about the initial states will be finally erased. The situation changes for incommensurate systems with strong quasidisorders (for example, $\Delta = 4$), where the occupation probabilities of the excitation decrease slowly, even if the initial state overlaps with the DBS or the BIC. Furthermore, a significant recurrence of survival probabilities for the excitation can be found when the initial state overlaps with neither the DBS nor the BIC. These two features may be understood as arising from the interplay between localizations in the system and the effective long-range correlation induced by the bath. Another important consequence of this interplay is the long-range hopping of the single excitation in the system, which causes the excitation hop to a different site from the initial one. We note that the hopping can also happen between two localized DBSs in commensurate cases, as shown for $\phi = 0.66\pi$ in Fig. 7(a).

An open question is the effect of interactions between atoms upon the prediction. Competition between interactions and disorder is known to be responsible for the many-body-localization transition in the AAH model [19]. Recall that the interatomic interaction may destroy the localization,

and the edge mode of the system can be changed. Moreover, the bound states in the open systems amount to an effective trap potential [20,21], which prevents the excitation from decaying. Hence, when interatomic interactions are involved, the competition between the effective trapping and the interatomic interactions is an interesting feature. When trapping is dominant, the excitation can be preserved in the system. Otherwise, the excitation dissipates. Due to the complicated and involved calculation for multiexcitation bound states [20], we leave the related discussion for future work.

APPENDIX A

In this Appendix, the exact energy solutions to Eq. (3) are presented for $\beta = p/q$ under the periodic boundary condition. Assume $N = Lq$, and then H_S can be written as

$$
H_S = \sum_{x=1}^{L} (c_1^\dagger, c_2^\dagger, \cdots, c_q^\dagger)_x
\begin{pmatrix}
\Delta \cos\left(\frac{2\pi p}{q} + \phi\right) & J & 0 & \cdots \\
J & \Delta \cos\left(\frac{4\pi p}{q} + \phi\right) & J & 0 \\
\vdots & \vdots & \ddots & \vdots \\
0 & \cdots & J & \Delta \cos(\phi)
\end{pmatrix}
\begin{pmatrix}
c_1 \\
c_2 \\
\vdots \\
c_q
\end{pmatrix}_x
$$

$$
+ \sum_{x=1}^{L} (c_1^\dagger, c_2^\dagger, \cdots, c_q^\dagger)_x
\begin{pmatrix}
0 & 0 & \cdots & 0 \\
\vdots & \ddots & \vdots & \vdots \\
1 & 0 & \cdots & 0
\end{pmatrix}
\begin{pmatrix}
c_1 \\
c_2 \\
\vdots \\
c_q
\end{pmatrix}_{x+1}
+ \text{H.c.}
\tag{A1}
$$

By Fourier transformation $c_x = \frac{1}{\sqrt{L}} \sum_{\lambda=1}^{L} a_\lambda e^{i2\pi\lambda x/L}$, we obtain

$$
H_S = \sum_{\lambda=1}^{L} (a_1^\dagger, a_2^\dagger, \cdots, a_q^\dagger)_\lambda
\begin{pmatrix}
\Delta \cos\left(\frac{2\pi p}{q} + \phi\right) & J & 0 & \cdots & e^{i2\pi q\lambda/L} \\
J & \Delta \cos\left(\frac{4\pi p}{q} + \phi\right) & J & 0 & \cdots \\
\vdots & \vdots & \ddots & \vdots & \vdots \\
e^{-i2\pi q\lambda/L} & 0 & \cdots & J & \Delta \cos(\phi)
\end{pmatrix}
\begin{pmatrix}
a_1 \\
a_2 \\
\vdots \\
a_q
\end{pmatrix}_\lambda .
$$

As for H_{int},

$$
H_{\text{int}} = \sum_{k,x} g_k b_k (c_1^\dagger, c_2^\dagger, \cdots, c_q^\dagger)_x + g_k^* b_k^\dagger
\begin{pmatrix}
c_1 \\
c_2 \\
\vdots \\
c_q
\end{pmatrix}_x
$$

$$
\Rightarrow \frac{1}{\sqrt{L}} \sum_k g_k b_k (a_1^\dagger, a_2^\dagger, \cdots, a_q^\dagger)_{\lambda=0} + g_k^* b_k^\dagger
\begin{pmatrix}
a_1 \\
a_2 \\
\vdots \\
a_q
\end{pmatrix}_{\lambda=0}
\tag{A2}
$$

For a single excitation, the eigenfunction $|\psi\rangle_E$ can be written for $\lambda = 0$ as

$$
|\psi\rangle_E = \left(\sum_{n=1}^{q} \alpha_n a_n^\dagger |0\rangle_n\right) \otimes |0\rangle^{\otimes M}
$$

$$
+ |0\rangle^{\otimes q} \left(\sum_{k=1}^{M} \beta_k b_k |0\rangle_k |0\rangle^{\otimes(M-1)}\right).
\tag{A3}
$$

When $p = 1$ and $q = 3$, we substitute Eq. (4) into Eq. (3), and eliminate the degree of freedom of the bath. One can obtain
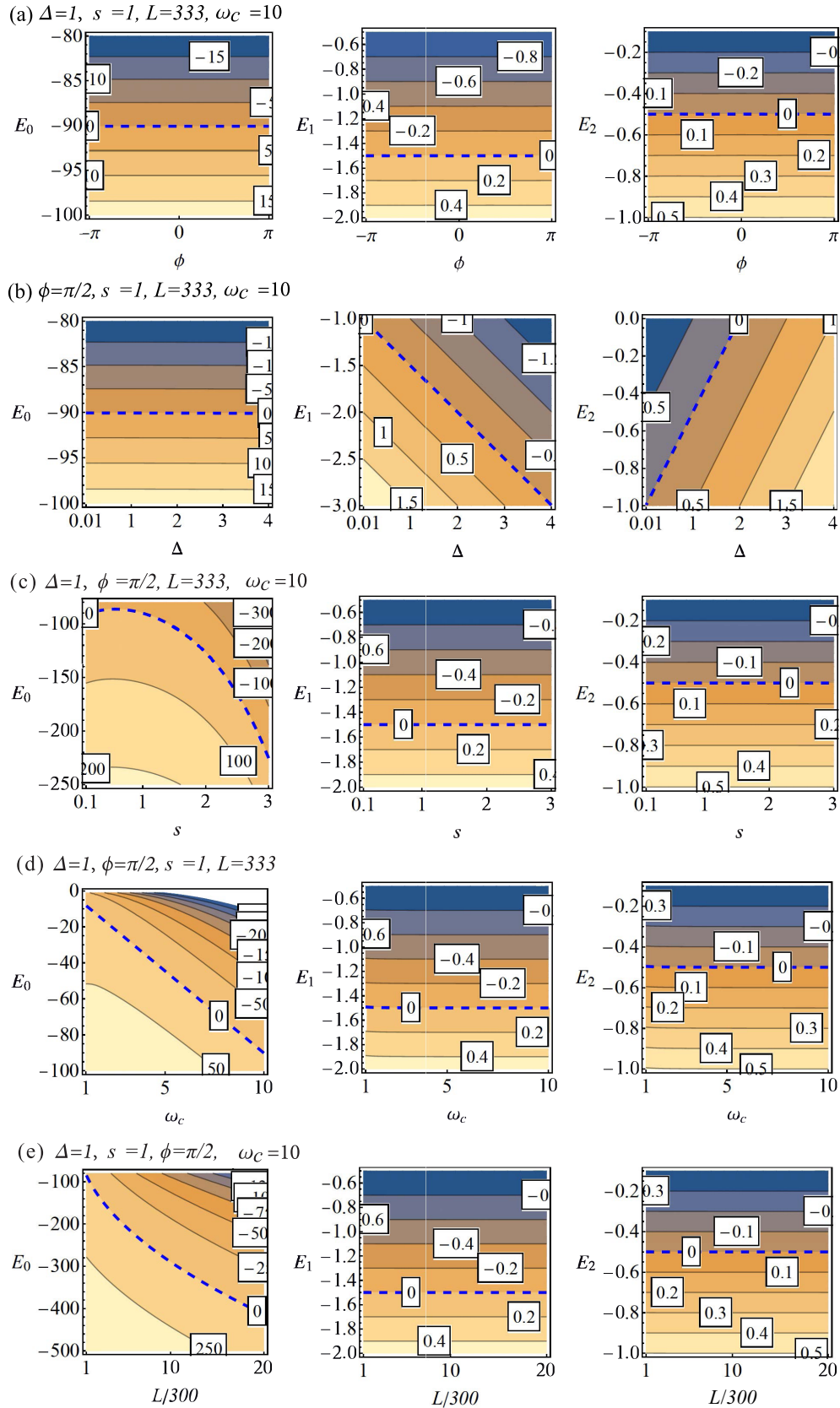
FIG. 9. The plots for Eqs. (A4) when $\beta = p/q$. The parameters are shown in the plot labels. $\eta = 0.1$ is chosen for all the plots.
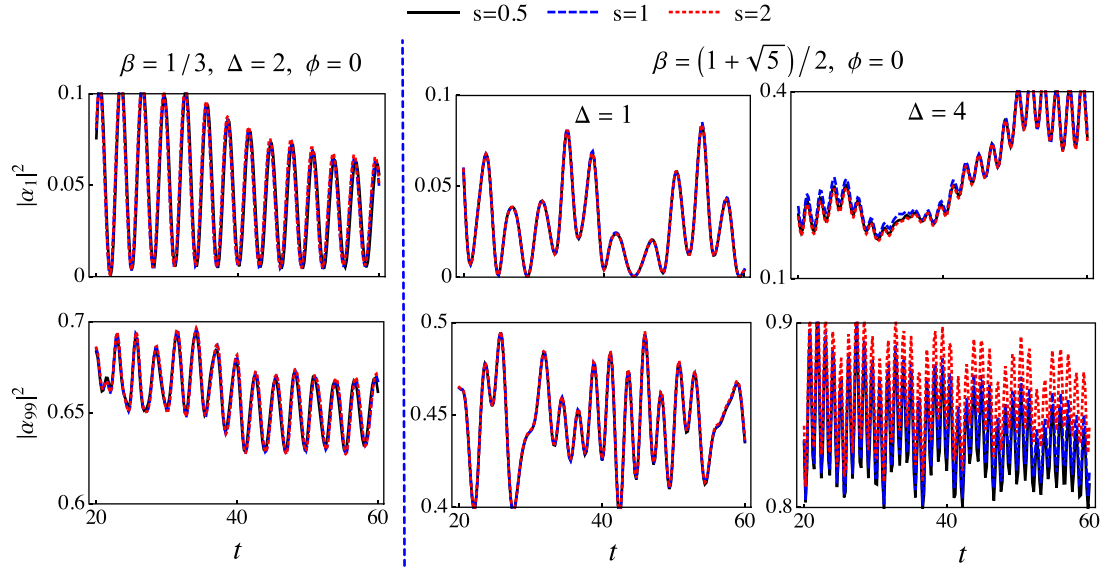
FIG. 10. The plots of survival probability $|\alpha_{1(99)}|^2$ vs s when $\Delta = 1/3$ and $(1 + \sqrt{5})/2$. The chosen parameters are shown in the plot label. $N = 99$, $\eta = 0.1$, $\omega_c = 10$ for all plots.

the equation

$$E^3 - 3d(E)E^2 - \left(3 + 6d(E) + \frac{3}{4}\Delta^2\right)E$$

$$- \left(2 + 3d(E) - \frac{3a}{4}\Delta^2 + \frac{\Delta^3}{4}\cos 3\phi\right) = 0,$$

where $d(E) = \frac{1}{L}\int_0^\infty \frac{J(\omega)}{E-\omega}d\omega$. By solving the above equation, three relations can be found:

$$E_0 = \sqrt{4[1 + d(E_0)]^2 + \Delta^2}\cos\left(\theta_\phi + \frac{2\pi}{3}\right) + d(E_0),$$

$$E_1 = \sqrt{4[1 + d(E_1)]^2 + \Delta^2}\cos\left(\theta_\phi + \frac{4\pi}{3}\right) + d(E_1),$$

$$E_2 = \sqrt{4[1 + d(E_2)]^2 + \Delta^2}\cos\theta_\phi + d(E_2), \quad \text{(A4)}$$

where

$$\theta_\phi = \frac{1}{3}\arccos\left\{\frac{[1 + d(E)]^3 + \frac{1}{8}\Delta^3\cos 3\phi}{\sqrt[3]{[1 + d(E)]^2 + \Delta^2/4}}\right\}. \quad \text{(A5)}$$

E_0, E_1, and E_2 are three real solutions, which are plotted for different parameters by dashed blue lines in Fig. 9. We

note that E_0 shows the significant dependence on the bath properties and the system size L, and thus is extensive. By contrast, both E_1 and E_2 are entirely determined by the system properties, and thus are intensive.

These solutions correspond to the three kinds of bound state in the main text: E_0 corresponds to the minimal solution to Eq. (8), which is extended and has a finite probability of spontaneous emission. By contrast, E_1 and E_2 correspond to the DBS. In Fig. 10, the excitation evolution for initial excitation at $n_0 = 1$ and 99 is plotted for different s. It is apparent that the survival probability is insensitive to the value of s.

APPENDIX B

The IPR is a measure for the localization of the state. Given $|\psi\rangle = \sum_{n=1}^N \alpha_n|n\rangle$, in which $|n\rangle$ denotes the occupation of the nth site, and N is the number of the site, the IPR is defined as

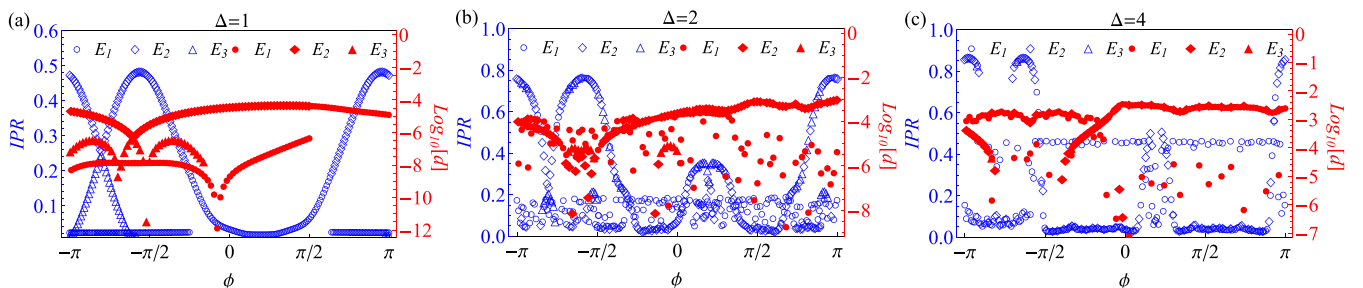$$\text{IPR}_\psi = \sum_{n=1}^N |\alpha_n|^4. \quad \text{(B1)}$$

FIG. 11. Plots of the IPR (blue empty symbols) and d (red solid symbols) for the DBS when $\beta = (1 + \sqrt{5})/2$ and $\Delta = 1, 2, 4$, respectively. The parameters are the same as those in Fig. 2. The labels of E_1, E_2, and E_3 denote the levels of the DBS, plotted in Fig. 2, in increasing order.
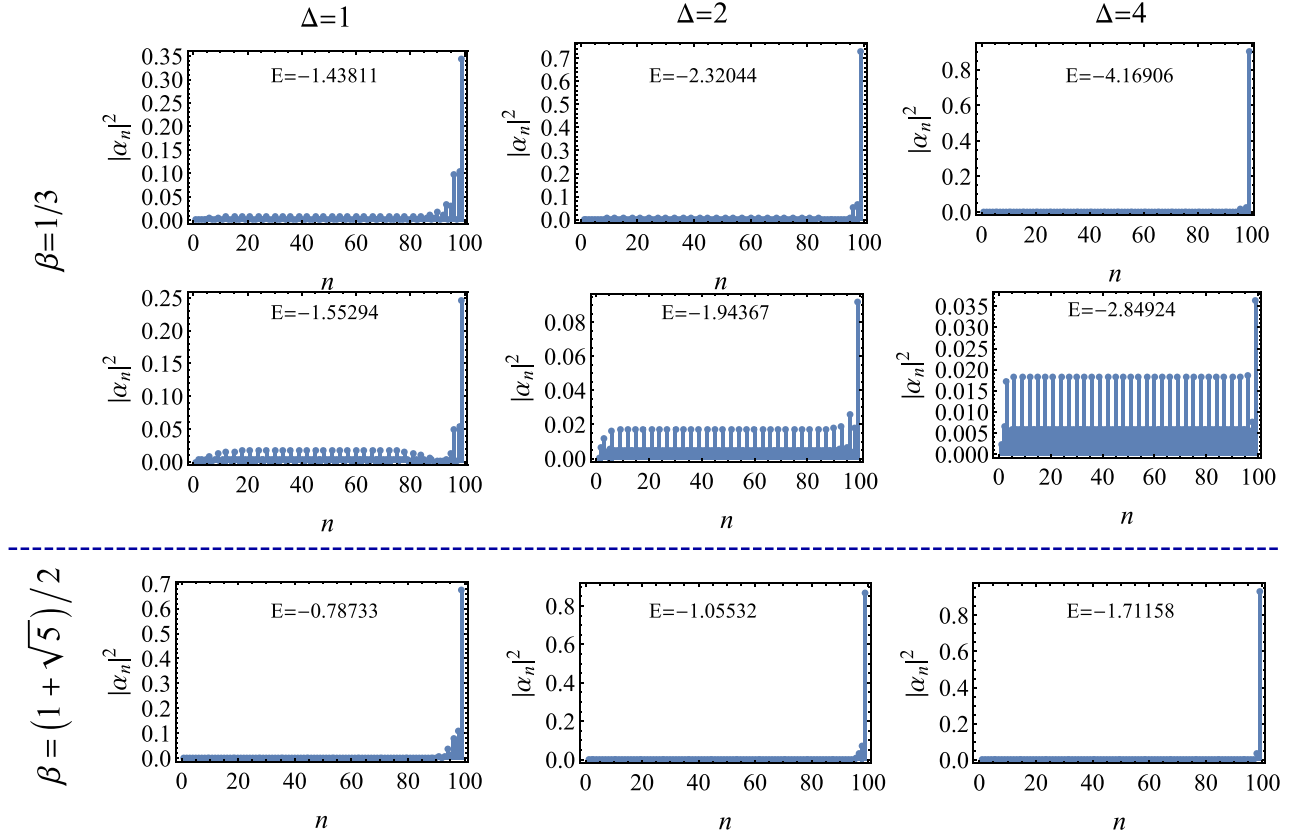
FIG. 12. The plots for the distribution $|\alpha_n|^2$ of the DBS when $\phi = -\pi$. Except for the values of β and Δ, the other parameters are the same as those in Fig. 3.

The IPR has the minimum $1/N$ only if $|\alpha_n|^2 = 1/N$ for arbitrary n, which means that the distribution of excitation is uniform, and thus the state is extended. However, the IPR has the maximum 1 only if $|\alpha_n|^2 = 1$ for a special n, which means that excitation can appear only at site n, and thus the state behaves localized strongly.

In Fig. 11, the IPR and corresponding d are plotted for different Δs when $\beta = (1 + \sqrt{5})/2$. Apparently the DBS is localized, and the corresponding IPR is enhanced with the increment of Δ.

We note that the IPR for the DBS is smaller than 1. The reason is the interplay between the localization, which tends to localize the excitation in the system, and the bath-induced long-range correlation in atomic sites, which tends to delocalize the excitation instead. In Fig. 12, the excitation distribution $|\alpha_n|^2$ for the DBS is shown for different Δ when $\phi = -\pi$. When $\beta = 1/3$, there are two DBSs: One corresponds to the renormalized edge state, and thus show strong localization. The other comes from the transition of the state in the band, and thus is extended. As for the first DBS, $|\alpha_n|^2$ becomes much pronounced at end site $n = 99$ with the increment of Δ, as shown in the upper row in Fig. 12. However, for the second one, $|\alpha_n|^2$ tends to be multipeaked with the increment of Δ, as shown in the middle row in Fig. 12. As a result, the localization of the DBS becomes enhanced with the increasing of Δ, as shown by the bottom row in Fig. 12.
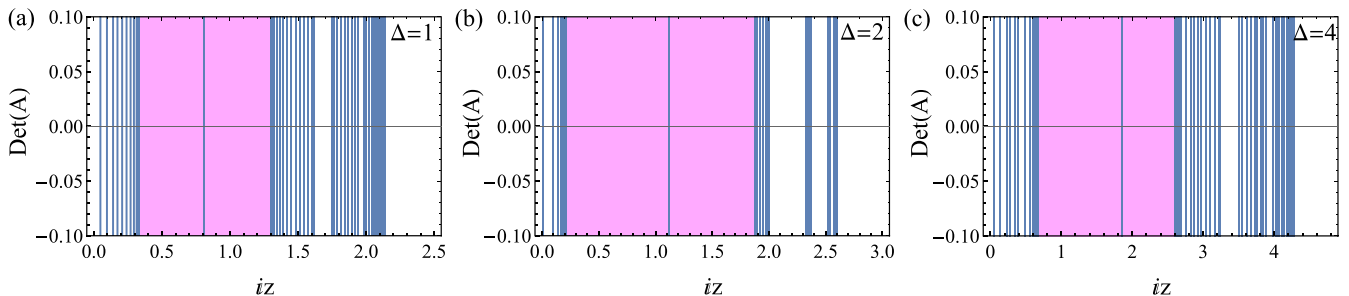

FIG. 13. The plots of Det(A) for $\beta = (1 + \sqrt{5})/2$, $\phi = 0.4\pi$ when $\Delta = 1, 2, 4$, respectively. $N = 99$, $s = 1$, $\eta = 0.1$, $\omega_c = 10$ are chosen for all plots. The region highlighted by dark-pink color denotes the main energy gap in Fig. 2.
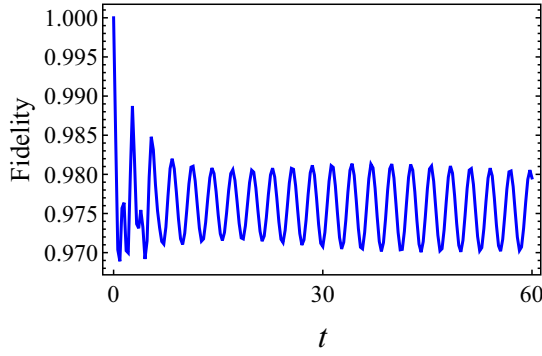
FIG. 14. The fidelity plotting for the time evolution of a special edge mode in H_S, which occurs at $\phi = 0$ and $\beta = 1/3$, $\Delta = 2$. The other parameters are the same as those in Fig. 3.

APPENDIX C

In this Appendix, we demonstrate the existence of the BIC in an analytical way. For this purpose, we first rewrite the system Hamiltonian as the diagonal form, $H_S = \sum_{i=1}^{N} \epsilon_i \eta_i^\dagger \eta_i$, in which $\eta_i = \sum_n \gamma_{in}^* c_n$. The array $(\gamma_{i1}, \gamma_{i2}, \cdots, \gamma_{iN})^T$ denotes the ith eigenstate of Eq. (1). Then the total Hamiltonian can be rewritten as

$$H = \sum_{i=1}^{N} \epsilon_i \eta_i^\dagger \eta_i + \sum_k \omega_k b_k^\dagger b_k + \sum_{i,k} g_{ik}^* \eta_i b_k^\dagger + g_{ik} \eta_i^\dagger b_k,$$

(C1)

where $g_{ik} = g_k \sum_n \gamma_{in}$. For $|\psi(t)\rangle = [\sum_i \alpha_i(t) \eta_i^\dagger |0\rangle_i] |0\rangle^{\otimes M} + |0\rangle^{\otimes N} [\sum_k \beta_k(t) b_k^\dagger |0\rangle_k]$, the evolution equation can be written as

$$i \frac{\partial \alpha_i(t)}{\partial t} = \alpha_i(t) \epsilon_i - i \left(\sum_n \gamma_{in}^* \right) \sum_j \left(\sum_n \gamma_{jn} \right)$$
$$\times \int_0^\tau d\tau \alpha_j(t) \sum_k |g_k|^2 e^{-i\omega_k t}$$
$$= \alpha_i(t) \epsilon_i - i \left(\sum_n \gamma_{in}^* \right) \sum_j \left(\sum_n \gamma_{jn} \right)$$
$$\times \int_0^\tau d\tau \alpha_j(t) \int_0^\infty J(\omega) e^{-i\omega t},$$

where we have assumed that the excitation is located initially in the system, and thus $\beta_k(0) = 0$. By Laplace transformation

$G_i(z) = \int_0^\infty dt \alpha_i(t) e^{-zt}$, the equation above is transformed into

$$(iz - \epsilon_i) G_i(z)$$
$$- \Sigma(z) \left(\sum_n \gamma_{in}^* \right) \sum_j \left(\sum_n \gamma_{jn} \right) G_j(z) = i \alpha_i(0), \quad \text{(C2)}$$

where $\Sigma(z) = \int_0^\infty \frac{J(\omega)}{iz - \omega}$ is the self-energy. Then we obtain the linear system of equations for $G_i(z)$, for which the solution can be expressed as

$$G_i(z) = \frac{\text{Det}(B_i)}{\text{Det}(A)}. \quad \text{(C3)}$$

The element of coefficients matrix A is $A_{ij} = (iz - \epsilon) \delta_{ij} - \Sigma(z)(\sum_n \gamma_{in}^*)(\sum_n \gamma_{jn})$, and B_i denotes the modified A with the ith column replaced by $(\alpha_1(0), \alpha_2(0), \cdots, \alpha_N(0))^T$.

Then the BIC corresponds to the pole of $G_i(z)$ with $iz > 0$, which can be determined by finding the solutions to $\text{Det}(A) = 0$. However, because of the appearance of the term $(\sum_n \gamma_{in}^*)(\sum_n \gamma_{jn})$, the determined real solution iz would be different from ϵ_i, as shown in Fig. 13. This picture is different from the single qubit case [7,22], in which the occurrence of the BIC is due to the level resonance. As an example, $\text{Det}(A)$ is plotted for positive iz with different Δ in Fig. 13, for which the integral $\Sigma(z)$ is decided by its principle value. It is clear that a single zero point can be found in the gap, as shown in Fig. 13. Furthermore, the corresponding values of iz are slightly different from the energies of the edge mode, which are 0.804 62, 1.101 76, and 1.826 22 for $\Delta = 1, 2, 4$, respectively. In addition, there are many continuous zero points, which construct a band.

Now we will show the correspondence between the BIC and the discrete zero point. By inverse Laplace transformation, $\alpha_i(t)$ can be determined. We choose the initial state as the edge state at $\phi = 0$ when $\beta = 1/3$, $\Delta = 2$ as an example, which corresponds to the 47th eigenstate of H_S. Then, by inverse Laplace transformation of $G_{47}(z)$, the contribution of the zero point at $iz = 2.307 52$ to the excitation evolution can be expressed as $\approx 0.9876 e^{-i2.307 52t} \eta_{47}^\dagger |0\rangle$. By comparison, the evolution for the edge mode as the initial state is shown in Fig. 14. Apparently the fidelity $|\langle \psi_{\text{edge}} | \psi(t) \rangle|^2$ shows a stable oscillation around $0.9876^2 \sim 0.975$. Thus, we have demonstrated the correspondence of the discrete pole of $G_i(z)$ and the BIC.

[1] P. W. Anderson, Absence of diffusion in certain random lattices, Phys. Rev. **109**, 1492 (1958).

[2] D. Basko, I. Aleiner, and B. Altshuler, Metal-insulator transition in a weakly interacting many-electron system with localized single-particle states, Ann. Phys. (NY) **321**, 1126 (2006); V. Oganesyan and D. A. Huse, Localization of interacting fermions at high temperature, Phys. Rev. B **75**, 155111 (2007).

[3] C. J. Turner, A. A. Michailidis, D. A. Abanin, M. Serbyn, and Z. Papić, Weak ergodicity breaking from quantum many-body

scars, Nat. Phys. **14**, 745 (2018); Quantum scarred eigenstates in a Rydberg atom chain: Entanglement, breakdown of thermalization, and stability to perturbation, Phys. Rev. B **98**, 155134 (2018).

[4] Luca D'Alessio, Y. Kafri, A. Polkovnikovb, and M. Rigol, From quantum chaos and eigenstate thermalization to statistical mechanics and thermodynamics, Adv. Phys. **65**, 239 (2016); C. Gogolin and J. Eisert, Equilibration, thermalisation, and the emergence of statistical mechanics in closed quantum systems,

Rep. Prog. Phys. **79**, 056001 (2016); T. Mori, T. N. Ikeda, E. Kaminishi, and M. Ueda, Thermalization and prethermalization in isolated quantum systems: A theoretical overview, J. Phys. B **51**, 112001 (2018).

[5] E. Yablonovitch, Inhibited Spontaneous Emission In Solid-State Physics And Electrincs, Phys. Rev. Lett. **58**, 2059 (1987); S. John and J. Wang, Quantum Electrodynamics Near A Photonic Band Gap: Photon Bound States And Dressed Atoms, *ibid.* **64**, 2418 (1990); Quantum optics of localized light in a photonic band gap, Phys. Rev. B **43**, 12772 (1991); S. John and T. Quant, Spontaneous emission near the edge of a photonic band gap, Phys. Rev. A **50**, 1764 (1994); Quantum Optical Spin-Glass State Of Impurity Two-Level Atoms In A Photonic Band Gap, Phys. Rev. Lett. **76**, 1320 (1996).

[6] A. G. Kofman, G. Kurizki, and B. Sherman, Spontaneous and induced atomic deay in photonic band structures, J. Mod. Opt. **41**, 353 (1994).

[7] C. W. Hsu, B. Zhe, A. Douglas Stone, J. D. Joannopoulos, and M. Soljačić, Bound state in the continuum, Nat. Rev. Mat. **1**, 16048 (2016).

[8] M. Schreiber, S. S. Hodgman, P. Bordia, H. P. Lüschen, M. H. Fishcher, R. Vosk, E. Altman, U. Schneider, and I. Bloch, Observation of many-body localization of interacting fermions in a quasirandom optical lattice, Science **349**, 842 (2015); P. Bordia, H. P. Lüschen, S. S. Hodgman, M. Schreiber, I. Bloch, and U. Schneider, Coupling Identical One-Dimensional Many-Body Localized Systems, Phys. Rev. Lett. **116**, 140401 (2016); P. Bordia, H. Lüschen, S. Scherg, S. Gopalakrishnan, Michael Knap, U. Schneider, and I. Bloch, Probing Slow Relaxation And Many-Body Localization In Two-Dimensional Quasiperiodic Systems, Phys. Rev. X **7**, 041047 (2017).

[9] H. P. Lüschen, P. Bordia, S. S. Hodgman, M. Schreiber, S. Sarkar, A. J. Daley, M. H. Fischer, E. Alman, I. Bloch, and U. Schneider, Signature Of Many-Body Localization In A Controlled Open Quantum System, Phys. Rev. X **7**, 011034 (2017).

[10] E. Levi, M. Heyl, I. Lesanovsky, and J. P. Garrahan, Robustness Of Many-Body Localization In The Presence Of Dissipation, Phys. Rev. Lett. **116**, 237203 (2016); M. H. Fischer, M. Maksymenko, and E. Altman, Dynamics of a Many-Body-Localized System Coupled to a Bath, *ibid.* **116**, 160401 (2016).

[11] L.-J. Lang, X. Cai, and S. Chen, Edge States And Topological Phases In One-Dimensional Optical Superlattice, Phys. Rev. Lett. **108**, 220401 (2012).

[12] S. Ya. Jitomirskaya, Metal-insulator transition for the almost Mathieu operator, Ann. Math. **150**, 1159 (1999).

[13] S. Aubry and G. André, Analyticity breaking and Anderson localization in incommensurate lattices, Ann. Isr. Phys. Soc. **3**, 133 (1980); P. G. Harper, Single band motion of conduction electrons in a uniform magnetic field, Proc. Phys. Soc. London, Sect. A **68**, 874 (1955).

[14] D. R. Hofstadter, Energy levels and wave functions of Bloch electrons in rational and irrational magnetic fields, Phys. Rev. B **14**, 2239 (1976); Y. E. Kraus, Y. Lahini, Z. Ringel, M. Verbin, and O. Zilberberg, Topological States And Adiabatic Pumping In Quasicrystals, Phys. Rev. Lett. **109**, 106402 (2012).

[15] B.-J. Yang, M. S. Bahramy, and N. Negaosa, Topological protection of bound state against the hybridization, Nat. Commn. **4**, 1524 (2013).

[16] Y.-X. Yao, G. Ma, Z.-Q. Zhang, and C. T. Chan, Topological Subspace-Induced Bound State In The Continuum, Phys. Rev. Lett. **118**, 166802 (2017).

[17] B. Fain, Relaxation via spontaneous emission of bosons: Non-Markovian approach, Phys. Rev. A **37**, 546 (1988).

[18] A. J. Leggett, S. Chakravarty, A. T. Dorsey, Matthew P. A. Fisher, A. Garg, and W. Zwerger, Dynamics of the dissipative two-state system, Rev. Mod. Phys. **59**, 1 (1987).

[19] S. Iyer, V. Oganesyan, G. Refael, and David A. Huse, Many-body localization in a quasiperiodic system, Phys. Rev. B **87**, 134202 (2013).

[20] T. Shi, Y.-H. Wu, A. González-Tudela, and J. I. Cirac, Bound States In Boson Impurity Models, Phys. Rev. X **6**, 021027 (2016).

[21] T. Shi, Y.-H. Wu, A. González-Tudela, and J. I. Cirac, Effective many-body Hamiltonian of qubit-photon bound states, New J. Phys. **20**, 105005 (2018).

[22] S. Longhi, Bound state in the continuum in a single-level Fano-Anderson model, Euro. Phys. J. B **57**, 45 (2007).